

The influence of H₂O on the viscosity of a haplogranitic melt

FRANK SCHULZE,¹ HARALD BEHRENS,¹ FRANÇOIS HOLTZ,² JACQUES ROUX,² AND WILHELM JOHANNES¹

¹Institut für Mineralogie, Universität Hannover, Welfengarten 1, D-30167 Hanover, Germany

²CRSCM-CNRS, 1A rue de la Férollerie, 45071 Orléans, France

ABSTRACT

The viscosity η of dry and hydrous haplogranitic melts (anhydrous normative composition: QZ₂₈Ab₃₄Or₃₈) has been determined between 3 and 10 kbar and 800 and 1400 °C using the falling-sphere method. The H₂O content of the melt ranged from 0.03 to 8.21 wt%. Experiments were performed in internally heated pressure vessels ($T = 900$ – 1400 °C) and cold-seal pressure vessels ($T = 800$ °C).

The viscosity decreases with increasing H₂O content of the melt. The strongest decrease is observed at low H₂O concentrations. The effect of H₂O is smaller at high H₂O concentrations in the melt, with an almost linear behavior between $\log \eta$ and H₂O content expressed as weight percent H₂O (decrease of 0.26 log units per weight percent H₂O for H₂O contents ≥ 4 wt% H₂O). No pressure effect could be observed between 3 and 10 kbar at 900 °C for a melt containing 5.90 wt% H₂O. In the investigated range the activation energy of the viscous flow decreases from 195 to 133 kJ/mol for melts with 1.05 to 8.21 wt% H₂O. The effect of T and H₂O content of the melt on viscosity can be calculated with a precision of ± 0.2 log units with the use of the following expression: $\log \eta = -1.57 + [23.398 - 13.197(c_{\text{H}_2\text{O}})^{0.11}] \times 10^3 (1/T)$.

Viscosities calculated using the model of Shaw (1972) show that, for the investigated composition, the model underestimates the influence of H₂O for low H₂O concentrations (≤ 4 wt% H₂O, difference up to two orders of magnitude at 800 °C) and overestimates slightly the influence of H₂O for high H₂O concentrations (≥ 5 wt% H₂O). In comparison with the model of Persikov et al. (1990), which takes into account the OH⁻ and molecular H₂O proportions, the experimental data at 800 °C are in good agreement with the calculated viscosities (deviation ≤ 1 log unit) assuming that the proportions of OH⁻ groups and molecular H₂O are those found in an in situ spectroscopic investigation of the melt. However, at higher temperatures (1000–1300 °C) the viscosity is overestimated for the OH⁻ and H₂O proportions recalculated for the appropriate temperatures.

INTRODUCTION

The viscosity of silicate liquids is one of the most important parameters controlling the behavior of magmas and the evolution of igneous rocks. It has been shown previously that H₂O can be a major constituent of natural magmas and has a pronounced influence on their physicochemical properties (e.g., Goranson 1938; Tuttle and Bowen 1958). In particular, H₂O reduces melt viscosity, which influences melt diffusivity and affects equilibrium-disequilibrium melting and crystallization processes (e.g., Watson 1994). The segregation of melts from protoliths and the ability of melts to ascend in the crust as diapirs or dikes are also directly related to the melt viscosity (e.g., Petford et al. 1993; Sawyer 1994).

Some previous experimental studies focused on the influence of H₂O on the viscosity of aluminosilicate liquids (Sabatier 1956; Shaw 1963; Friedman et al. 1963; Burnham 1964; Kushiro 1978a; Dingwell and Mysen 1985; Dingwell 1987; Persikov et al. 1990; White and Montana

1990; Baker and Vaillancourt 1995). All these studies showed that viscosity decreases strongly with the addition of H₂O to the melt, which is usually interpreted as a consequence of melt depolymerization (see, however, controversial interpretation for albite melt in Kohn et al. 1989).

Spectroscopic investigations indicate that H₂O in silicate melts is incorporated as hydroxyl units (OH⁻ groups) and molecular H₂O (e.g., Stolper 1982; Silver and Stolper 1989; Nowak and Behrens 1995). It is assumed that the incorporation of the OH⁻ groups is mainly responsible for the decrease in viscosity, whereas molecular H₂O has a minor effect on the viscosity (e.g., Stolper 1982; Persikov et al. 1990). However, the individual effects of OH⁻ groups and molecular H₂O are not well known. This is mainly because few studies have focused on the effect of low concentrations of H₂O on melt viscosity. Most of the available data are for H₂O contents > 2 wt%. In this study the influence of H₂O on the viscosity of a haplogranitic melt was investigated within a wide range of H₂O con-

tent, temperature, and pressure. Some petrogenetic implications are discussed.

Models for the calculation of viscosity on the basis of melt composition were developed by several workers (Shaw 1972; Bottinga and Weill 1972; Richet 1984; Persikov et al. 1990). The results of this investigation are compared with viscosities calculated using the models of Shaw (1972) and Persikov et al. (1990) because these are the only ones that consider the influence of H₂O on melt viscosities.

EXPERIMENTAL METHODS

Starting material and analytical techniques

Starting material for the viscosity experiments was a dry haplogranitic glass (labeled AOQ) with a composition close to the 2 kbar ($p_{\text{H}_2\text{O}}$) ternary minimum composition in the system SiO₂-NaAlSi₃O₈-KAlSi₃O₈-H₂O. The glass was prepared by the German company Schott (melt no. N8886) by fusion of oxide and carbonate powders. The composition of the dry glass was analyzed by electron microprobe as 76.12 wt% SiO₂, 13.53 wt% Al₂O₃, 4.65 wt% Na₂O, and 5.68 wt% K₂O (Q_{Z28}Ab₃₄Or₃₈, normative proportions). This composition is the same as that used in investigations on H₂O solubility (Holtz et al. 1992, 1995, composition labeled SCHOTT and AOQ, respectively), H₂O diffusion (Nowak and Behrens 1992), and H₂O speciation at high *P* and *T* (Nowak 1995; Nowak and Behrens 1995). The H₂O-bearing glasses were synthesized by high-pressure fusion of H₂O plus glass powder. Known amounts of doubly distilled water were added to 0.8–1.2 g of powdered glass (grain size <500 μm) and sealed in 6 mm diameter, 30 mm long platinum capsules. The glasses were fused in an internally heated pressure vessel (IHPV) at 5 kbar and 1200 °C for approximately 72 h. By this procedure bubble-free glass bodies with H₂O contents from 1.05 to 8.21 wt% H₂O were synthesized (see Table 1).

The H₂O contents of the starting glasses were determined by Karl-Fischer titration (KFT) and by Fourier-transform infrared (FTIR) spectroscopy on some samples (see Table 1). The analytical precision obtained from KFT depends mainly on the amount of glass and the duration of the measurement. In the case of this study the precision is within ±0.10 wt% H₂O (for more details on KFT, see Holtz et al. 1992; Behrens 1995). The homogeneous distribution of H₂O was tested by analyzing the H₂O content by KFT at both ends of the starting glass bodies. The results (Table 1) show that except for sample AOQVis5 the H₂O is homogeneously distributed within the glass. In the case of sample AOQVis5 a homogeneous H₂O distribution should have been reached within the first viscosity experiment, considering average diffusion coefficient of H₂O of about 10⁻⁷ cm²/s at 850 °C (Lapham et al. 1984; Nowak and Behrens 1992). For each sample the H₂O content is considered to be the average value of KFT determinations.

In some samples the distribution of H₂O was checked

by FTIR spectroscopy (Bruker IFS 88) before and after the experiments (see Table 1). The measurements were performed in a chamber purged with dry air. The spacial resolution was 1 mm. The H₂O contents of the glasses were determined by measuring the heights of the absorption band near 7050 cm⁻¹ (first overtone band of O-H stretching mode; Stolper 1982). This band was chosen because the measurements could be directly performed on the glass cylinders (diameter 4 mm) used in the viscosity experiments. The linear molar absorptivity for the 7050 cm⁻¹ band was determined to be 0.241 L/(mol·cm) by using reference samples analyzed by KFT (Behrens et al., in preparation). The density of the reference samples is given by $\rho_{g/1} = 2347 - 12.6(c_{\text{H}_2\text{O}})$. The uncertainty on the H₂O contents measured by FTIR spectroscopy is believed to be within ±10% (relative).

Sample preparation for viscosity measurements

Viscosity measurements by the falling-sphere method require the determination of the exact position of the sphere in the glass cylinder before and after the experiment. Therefore, a marker used as reference point for distance measurements had to be incorporated into the glass. The first-step experiments consisted of the preparation of glass cylinders containing a marker and platinum spheres. The following procedure was used.

Cylinders of 3.8 mm in diameter and about 16 mm in length were cored from the starting glass bodies. One slice of about 1–2 mm thickness was cut off from these cylinders. Platinum capsules (4 mm diameter, 0.2 mm wall thickness) were welded at one end and gently deformed to fit exactly with the cored glass. A small amount of crushed glass with the same H₂O content as the cylinder was put at the bottom of the capsule. Then the thin slice of glass and the glass cylinder were inserted. A very small amount of platinum powder placed between the slice and the cylinder was used as a marker for the later measurement of the sphere position. On top of the cylinder a small amount of powder was tightly packed with one or two platinum spheres made by the method of Hazen and Sharpe (1983). The capsule was finally welded at the other end. In experiments with two spheres care was taken to avoid contact between spheres. The radii of the platinum spheres were measured under the microscope with a graduated eye-piece to ±5 μm. Radii of the spheres used in the experiments varied between 0.095 and 0.172 mm. The samples were then brought to *P-T* conditions (for experimental apparatus and conditions, see below) and the spheres started to fall into the glass cylinder. No viscosity determination could be made from this first step because of the undefined starting position of the sphere within the powder.

In the second-step experiments, viscosity data were collected by measuring the position of the spheres relative to the marker before and after the experiment. The exact position of the spheres relative to the platinum marker could be measured using an optical microscope. The microscope is equipped with an *x-y* stage that enables dis-

tance measurements with a precision of 10 μm . The cylinder was placed in a small glass container filled with a mixture of quinoline and glycerol, which had the same refractive index as the glass. The container was covered with a thin plate of glass in direct contact with the liquid to provide a plane surface. This setup led to perfect visibility of the platinum marker and the sphere under the microscope because any disturbing influence of the glass body (e.g., roughness of the surface, optical effect resulting from the cylindrical shape) could be avoided. After measuring the sphere position the samples were again placed in platinum capsules, which were then welded at both ends. By bringing the sample to the experimental conditions the spheres settled within the melt. After the experiment the capsule was removed and the sphere position was measured again as described above.

For the following experiment the glass cylinder was turned upside down, allowing the spheres to settle toward the opposite direction. By this procedure up to ten experiments were performed with each sample.

Experimental apparatus

Experiments at 800 °C and 5 kbar were performed in a vertical cold-seal pressure vessel (CSPV) with H₂O as a pressure medium. Temperature was measured with an NiCr-Ni thermocouple calibrated against a certified thermocouple. The actual temperature was believed accurate to within ± 8 °C. Pressure was measured with a strain gauge manometer (for details on the CSPV, see Puziewicz and Johannes 1988). The heating rate was about 60 °C/min. Samples were quenched isobarically with a flux of compressed air resulting in an initial quench rate of 250 °C/min. Experimental durations varied between 7 and 71 h. Uncertainties in the estimation of the effective duration (settling time of the sphere) owing to the heating and cooling period are about ± 4 min (equal to a maximum uncertainty of $\pm 1\%$ for the settling time of the spheres).

The experiments at temperatures above 800 °C were performed in two IHPVs with argon as the pressure medium. The type I vessel was used for high-pressure experiments (up to 10 kbar at 900 °C) and the type II vessel for high-temperature experiments (1000–1400 °C at 3 kbar). For both types of vessels the samples were pressurized to 60% of the final pressure, and the experimental pressure was reached during heating. For type I, working with a furnace made of Kanthal wires, heating was performed in one step with a heating rate of 120 °C/min. The temperature was controlled with a Pt-PtRh10 thermocouple at the top and a PtRh10-PtRh30 thermocouple at the bottom of the capsule. For type II, working with a furnace made of Kanthal and platinum wires, heating was performed in two steps (a detailed description of the furnace is given by Roux et al. 1994). First, the sample was preheated to 750 °C using the Kanthal resistors, and then, in the second step, the temperature was raised to the final experimental temperature by using the platinum resistor. For the second step the maximum heating rate was 160

TABLE 1. H₂O contents and density of glasses used in the viscosimetry experiments

| Sample | H ₂ O content* | | | | | Density (g/cm ³) |
|-----------|---|-----------------|----------|---|------------------------------|------------------------------|
| | wt% H ₂ O by KFT (starting material) | | Avg. KFT | wt% H ₂ O by IR spectroscopy | | |
| | A | B | | b.e. | a.e. | |
| AOQVis8 | 8.25 \pm 0.10 | 8.18 \pm 0.10 | 8.21 | 8.06 8.16 8.06 8.02 | 8.01 8.04 8.05 8.02 | 2.246 |
| AOQVis7 | 7.03 \pm 0.08 | 7.04 \pm 0.08 | 7.03 | 7.15 | n.d. | 2.257 |
| AOQVis6 | 6.11 \pm 0.08 | 5.71 \pm 0.08 | 5.90 | 6.19 6.20 | n.d. | 2.268 |
| AOQVis5 | 4.72 \pm 0.08 | 5.29 \pm 0.08 | 5.00 | 5.11 5.14 5.27 | 5.34 5.31 5.29 | 2.299 |
| AOQVis4 | 3.74 \pm 0.09 | 3.76 \pm 0.08 | 3.75 | n.d. | 4.07 4.09 4.07 3.94 | 2.310 |
| AOQVis3 | 3.17 \pm 0.08 | 3.28 \pm 0.06 | 3.22 | n.d. | 3.10 3.07 3.02 3.05 | 2.337 |
| AOQVis2.5 | 2.52 \pm 0.07 | 2.64 \pm 0.08 | 2.58 | n.d. | 2.70 2.65 2.66 2.69 | 2.342 |
| AOQVis2 | 2.08 \pm 0.07 | 2.12 \pm 0.08 | 2.10 | n.d. | 2.30 2.25 2.23 2.24 | 2.348 |
| AOQVis1.5 | 1.49 \pm 0.07 | 1.61 \pm 0.06 | 1.56 | n.d. | 1.75 1.75 1.74 1.69 | 2.347 |
| AOQVis1 | 0.96 \pm 0.03 | 1.16 \pm 0.07 | 1.05 | n.d. | 1.66 1.21 1.12 1.12 | 2.394 |
| AOQVis0 | 0.03 | n.d. | 0 | n.d. | n.d. | 2.359 |

Note: A and B were KFT measurements performed with glass pieces taken from ends of the starting glass bodies (for details, see text); b.e. = before experiments (starting material), a.e. = after experiments, and n.d. = not determined.

* To calculate in mole percent H₂O, the molecular weight on a one O atom basis for AOQ composition is 32.6 g.

°C/min. The temperature distribution was monitored with five PtRh10-PtRh30 thermocouples. One of them was at the top and another at the bottom of the capsule. For both IHPVs the temperature control was accurate to ± 15 °C. The observed temperature gradients along the sample were < 15 °C. Experimental durations varied between 1 and 46 h (Table 2). For both vessels quenching was performed by turning off the power supply, resulting in an initial quench rate of 120 °C/min. Uncertainties for the settling time of the sphere are ± 5 min for type I, and this results in an uncertainty of $\pm 3\%$ for settling time for the shortest experimental duration. For type II the uncertainty for the settling time is ± 3 min. This results in a maximal uncertainty of $\pm 5\%$ for settling time for 1 h experiments. Most experiments were performed for longer durations (Table 2) leading to smaller uncertainties.

TABLE 2. Experimental conditions and results

| T (°C) | P (bars) | Sphere radius (×10 ⁻² cm) | Exp. t (s) | Velocity (×10 ⁻⁵ cm/s) | log η (dPa·s) |
|--|----------|--------------------------------------|------------|-----------------------------------|---------------|
| AOQVis8 8.21 wt% H₂O | | | | | |
| 800 | 5000 | 1.48 | 51 870 | 1.625 | 4.68 |
| | | 1.48 | 25 100 | 1.647 | 4.67 |
| | | 1.38 | 25 100 | 1.275 | 4.72 |
| 900 | 5000 | 1.03 | 18 710 | 3.014 | 4.12 |
| | | 0.95 | 18 710 | 2.512 | 4.13 |
| AOQVis7 7.03 wt% H₂O | | | | | |
| 800 | 5000 | 1.57 | 83 590 | 0.732 | 5.07 |
| | | 1.57 | 74 180 | 0.891 | 4.98 |
| 900 | 5000 | 1.35 | 9 610 | 2.101 | 4.49 |
| | | 1.25 | 9 610 | 1.831 | 4.49 |
| | | 1.35 | 14 400 | 2.514 | 4.41 |
| | | 1.25 | 14 400 | 2.201 | 4.49 |
| | | 1.35 | 18 000 | 2.383 | 4.44 |
| | | 1.25 | 18 000 | 2.100 | 4.43 |
| AOQVis6 5.90 wt% H₂O | | | | | |
| 800 | 5000 | 1.54 | 246 040 | 0.460 | 5.26 |
| | | 1.48 | 249 540 | 0.438 | 5.24 |
| | | 1.48 | 51 100 | 0.218 | 5.26 |
| 900 | 3000 | 1.48 | 30 810 | 1.496 | 4.71 |
| | | 5000 | 43 900 | 1.822 | 4.63 |
| | | 7500 | 33 240 | 1.549 | 4.69 |
| 1000 | 3000 | 1.48 | 32 900 | 1.594 | 4.69 |
| | | 1.48 | 3 720 | 5.027 | 4.18 |
| AOQVis5 5.00 wt% H₂O | | | | | |
| 900 | 5000 | 1.36 | 81 260 | 0.667 | 4.99 |
| | | 1.44 | 81 260 | 0.735 | 5.00 |
| | | 1.36 | 75 180 | 0.632 | 4.89 |
| | | 1.44 | 75 180 | 0.924 | 4.89 |
| 1000 | 3000 | 1.36 | 14 260 | 2.664 | 4.39 |
| | | 1.44 | 14 260 | 2.902 | 4.40 |
| | | 1.36 | 22 540 | 2.945 | 4.34 |
| | | 1.44 | 22 540 | 3.233 | 4.35 |
| | | 1.36 | 26 640 | 2.920 | 4.35 |
| | | 1.44 | 26 640 | 3.202 | 4.36 |
| 1150 | 3000 | 1.36 | 3 300 | 11.136 | 3.77 |
| | | 1.44 | 3 300 | 12.258 | 3.78 |
| | | 1.36 | 3 600 | 12.139 | 3.73 |
| | | 1.44 | 3 600 | 13.250 | 3.74 |
| AOQVis4 3.75 wt% H₂O | | | | | |
| 1300 | 3000 | 1.18 | 3 660 | 16.462 | 3.52 |
| | | 1.23 | 3 660 | 13.470 | 3.57 |
| AOQVis3 3.22 wt% H₂O | | | | | |
| 1200 | 3000 | 0.96 | 14 200 | 1.831 | 4.27 |
| 1300 | 3000 | 0.96 | 3 000 | 4.467 | 3.88 |
| | | 0.96 | 5 970 | 4.858 | 3.85 |
| | | 1.55 | 5 970 | 5.846 | 3.91 |
| AOQVis2.5 2.58 wt% H₂O | | | | | |
| 1300 | 3000 | 1.18 | 9 890 | 4.325 | 4.07 |
| | | 1.18 | 4 330 | 4.315 | 4.07 |
| AOQVis2 2.09 wt% H₂O | | | | | |
| 1200 | 3000 | 1.18 | 72 600 | 1.237 | 4.61 |
| 1300 | 3000 | 1.27 | 14 490 | 3.499 | 4.22 |
| | | 1.18 | 14 490 | 3.225 | 4.19 |
| | | 1.18 | 14 400 | 3.267 | 4.19 |
| AOQVis1.5 1.55 wt% H₂O | | | | | |
| 1200 | 3000 | 1.65 | 39 690 | 1.315 | 4.85 |
| | | 1.55 | 39 690 | 1.153 | 4.85 |
| 1300 | 3000 | 1.65 | 21 000 | 3.352 | 4.44 |
| | | 1.55 | 21 000 | 2.955 | 4.45 |
| 1400 | 3000 | 1.65 | 6 210 | 9.372 | 3.97 |
| | | 1.55 | 6 210 | 8.010 | 3.98 |
| AOQVis1 1.05 wt% H₂O | | | | | |
| 1200 | 3000 | 1.67 | 118 260 | 0.581 | 5.21 |
| | | 1.60 | 118 260 | 0.532 | 5.21 |
| 1300 | 3000 | 1.67 | 28 320 | 1.631 | 4.77 |
| | | 1.60 | 28 320 | 1.501 | 4.77 |

TABLE 2.—Continued

| T (°C) | P (bars) | Sphere radius (×10 ⁻² cm) | Exp. t (s) | Velocity (×10 ⁻⁵ cm/s) | log η (dPa·s) |
|--|----------|--------------------------------------|------------|-----------------------------------|---------------|
| AOQVis0 0.03 wt% H₂O | | | | | |
| 1400 | 3000 | 1.69 | 165 660 | 0.102 | 5.91 |
| | | 1.72 | 165 660 | 0.111 | 5.92 |

Note: In the case of different sphere radii and the same experimental durations, one glass cylinder contained both spheres (one experiment yielded two viscosity determinations). Maximal uncertainties are as follows: $T \pm 15^\circ\text{C}$, $P \pm 50$ bars, sphere radius $\pm 5 \mu\text{m}$, velocity $\pm 5\%$, viscosity $\pm 15\%$.

Evaluation of the viscosity

The settling velocity data derived from the sphere position vs. time were related to the viscosity of the melt by Stokes law:

$$\eta = \frac{2r^2g\Delta\rho}{9\nu} C_F \quad (1)$$

where η is the viscosity, ν is settling velocity, $\Delta\rho$ is the density contrast between the sphere and the melt, g is the acceleration due to gravity, and r is the sphere radius. C_F is the Faxen correction, which takes into account the effects of viscous drag exerted on the settling sphere by the capsule walls (Faxen 1923; Shaw 1963) and is given by the equation

$$C_F = 1 - 2.104\left(\frac{r}{R}\right) + 2.09\left(\frac{r}{R}\right)^3 - 0.95\left(\frac{r}{R}\right)^5 \quad (2)$$

where R is the inner radius of the capsule.

The values used for calculating $\Delta\rho$ are the densities of Pt and the hydrous glasses at 1 atm. The density for Pt is 21.45 g/cm³ (Weast et al. 1984); the density of the hydrous glasses was measured on the glass bodies using the buoyancy method. The values for the density of the hydrous glasses are given in Table 1. Measurements performed on standard materials (e.g., quartz) proved the maximum uncertainties of the densities of the hydrous glasses to be within $\pm 1\%$. No correction was made for differential compression and thermal expansion because this would have only a small effect on $\Delta\rho$ (the density differences between the glass and the melt can be neglected; see Dingwell and Mysen 1985).

RESULTS AND DISCUSSION

The results of the falling-sphere experiments on the dry and hydrous AOQ melts along with the experimental parameters are listed in Table 2. Figure 1 presents the results in a plot of viscosity (expressed as $\log \eta$) vs. H₂O content of the melt (expressed as weight percent H₂O). In most experiments two spheres of different radii were used. To show that there is no interdependence between the two spheres, two sets of experiments with the same sample (AOQVis3) were performed under the same P - T conditions (3 kbar, 1300 °C). In the first set of experiments one sphere was added (sphere radius = 0.96×10^{-2} cm), and the measured viscosity was $10^{3.88}$ dPa·s. In the sec-

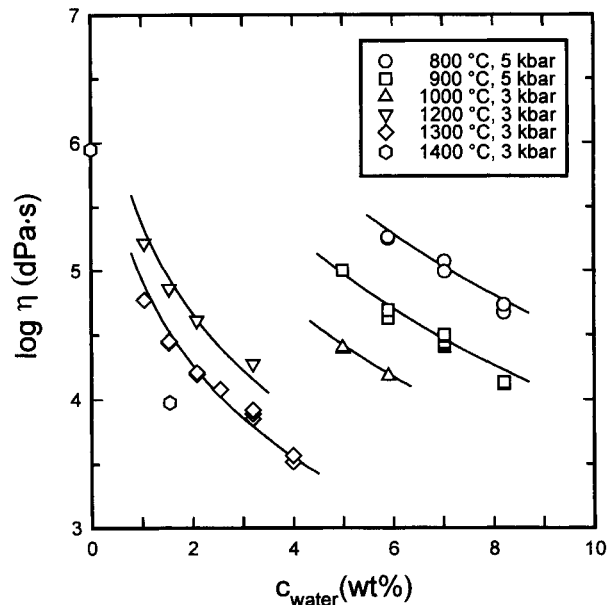


FIGURE 1. Results from viscosimetry experiments expressed as $\log \eta$ vs. total H₂O content of the investigated haplogranitic composition. Note that the results for 800 and 900 °C were obtained at 5 kbar, whereas the results at high temperature (1000–1400 °C) were obtained at 3 kbar. The symbol size represents the maximum uncertainty of $\pm 15\%$. The curves were calculated from Equation 5.1 (see text for explanation).

ond set of experiments a second sphere was added (radius = 1.55×10^{-2} cm). The viscosities from the second set of experiments ($10^{3.85}$ and $10^{3.91}$ dPa·s, calculated using the settling distance of the first and the second sphere, respectively) were found to be identical within error with the viscosity measured in the first set of experiments.

The experimental setup used in this study allowed the multiple use of one sample under various conditions. A possible source of errors would be a change in composition, especially loss of H₂O during sample preparation or experimentation. This was checked with a sample containing 5.90 wt% H₂O (AOQVis6) by reproducing the experimental conditions of the first experiment (800 °C, 5000 bars) after a series of eight experiments under various *P-T* conditions. The measured viscosities for the first and the last experiment were identical ($\log \eta = 5.26$, see Table 2). In addition, the H₂O contents of the glass cylinders were determined for most samples after the last viscosity measurement by IR spectroscopy (Table 1). The maximum difference between the H₂O content of the starting material and the H₂O content after the series of experiments was 0.3 wt% H₂O, which is within the uncertainty of the measurements (KFT and IR spectroscopy).

Pressure dependence of viscosity in hydrous melts

The pressure dependence of melt viscosity was studied for composition AOQVis6 at pressures of 3, 5, 7.5, and 10 kbar and the temperature of 900 °C. Figure 2 shows

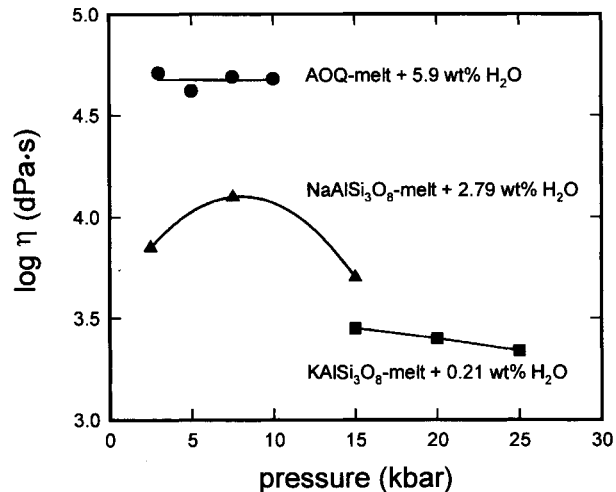


FIGURE 2. Pressure dependence of the AOQ melt containing 5.90 wt% H₂O (circles). Additional data are given for hydrous NaAlSi₃O₈ melt (triangles, Dingwell 1987) and hydrous KAlSi₃O₈ melt (squares, White and Montana 1990).

that within the experimental error no pressure dependence of the melt viscosity was observed. This suggests that all results obtained in this study at 3 and 5 kbar can be applied to the pressure range 3–10 kbar. Very low viscosity variations between 15 and 25 kbar were also obtained by White and Montana (1990) in KAlSi₃O₈ melt containing 0.2 wt% H₂O. It must be noted that the viscosity maximum reported by Dingwell (1987) at 7.5 kbar in albite melt with 2.8 wt% H₂O was not observed for our composition.

Dry melt

Because of the restricted range of viscosities that could be determined in this study (range of $\log \eta$ of 3.0–6.0) the viscosity of the dry melt could be determined only at the temperature of 1400 °C (at 3 kbar), with a value of $10^{5.91}$ dPa·s. To get an idea of anhydrous melt viscosities at lower temperatures, the result obtained at 1400 °C can be compared with measurements made at 1 atm by Dingwell et al. (1992) on a melt labeled HPG8. This composition (Qz₃₆Or₂₅Ab₃₉, normative composition) is slightly different from the AOQ composition in this study. Fit parameters given by Dingwell et al. (1992) for an Arrhenius equation were used to calculate the viscosity of HPG8 at 1400 °C. Because the viscosities for both melts were determined at different pressures, the effect of the pressure on the dry melt viscosity was taken into account. If we assume a similar pressure dependence of the viscosity of the anhydrous AOQ melt as determined for NaAlSi₃O₈ melt (Kushiro 1978b), the viscosity at 3 kbar should be about 17% lower than the viscosity at 1 bar. The calculated viscosity of HPG8 is $10^{5.94}$ dPa·s, which is identical within error limits to the measured value for the AOQ melt. In the following discussion we use the viscosities of the HPG8 melt at different temperatures as reference viscosities for the anhydrous AOQ melt for which viscosity

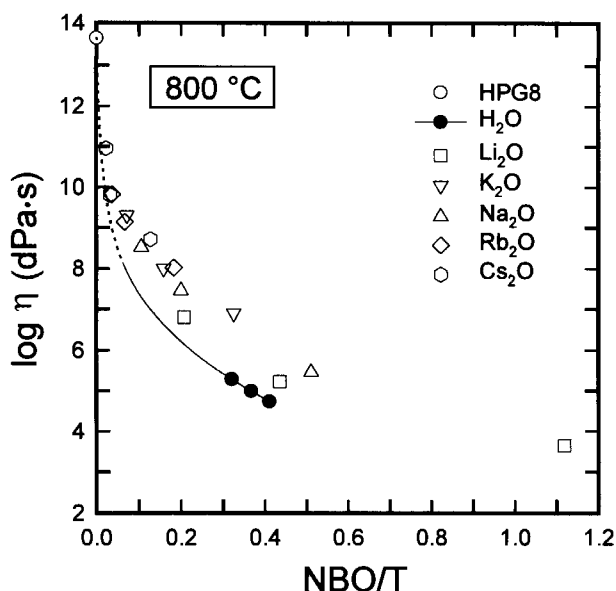


FIGURE 3. Comparison of the effect of H₂O on the viscosity of AOQ melt (this study) and the effect of alkali oxides on the viscosity of HPG8 melt (Hess et al. 1995). The solid circles represent viscosities from this study measured at 800 °C, 5 kbar. The curve for hydrous AOQ melt was calculated from Equation 5, the dashed part represents subsolidus conditions. Viscosities of the HPG8 + excess alkali melts were calculated with fit parameters given by Hess et al. (1995).

could not be measured at $T < 1400$ °C with the falling-sphere method.

Effect of H₂O

The viscosity of the melt decreases strongly with the addition of H₂O to the melt. By adding 1.5 wt% H₂O to the melt, the viscosity of the melt at 1400 °C and 3 kbar decreases by almost two orders of magnitude from $10^{5.91}$ dPa·s for the anhydrous melt to $10^{3.97}$ dPa·s for the hydrous melt. This decrease of viscosity with increasing H₂O content is more pronounced at low than at high temperature. At 1200 °C and 3 kbar the addition of 1 wt% H₂O to a dry melt leads to a decrease in viscosity of about 2.5 orders of magnitude, whereas at 1000 °C (T of dry solidus) a decrease of almost four orders of magnitude is expected (extrapolated). With the incorporation of higher amounts of H₂O into the melt, the decrease in viscosity is lower than at low H₂O contents. For instance, with the addition of 2 wt% H₂O to the anhydrous melt at 1300 °C the viscosity ($10^{4.20}$ dPa·s) decreases by 2.6 orders of magnitude. With the further addition of 2 wt% H₂O (4 wt% total H₂O) the viscosity decreases by 0.7 orders of magnitude ($10^{3.55}$ dPa·s). At high H₂O concentrations (>4 wt%) the decrease in viscosity expressed as $\log \eta$ shows a linear dependence on the H₂O concentration with the same slope (0.26 log units per weight percent H₂O) at all measured temperatures, whereas at low H₂O concentrations this decrease is strongly nonlinear. The strong nonlinear dependence of viscosity on the concentration of H₂O is

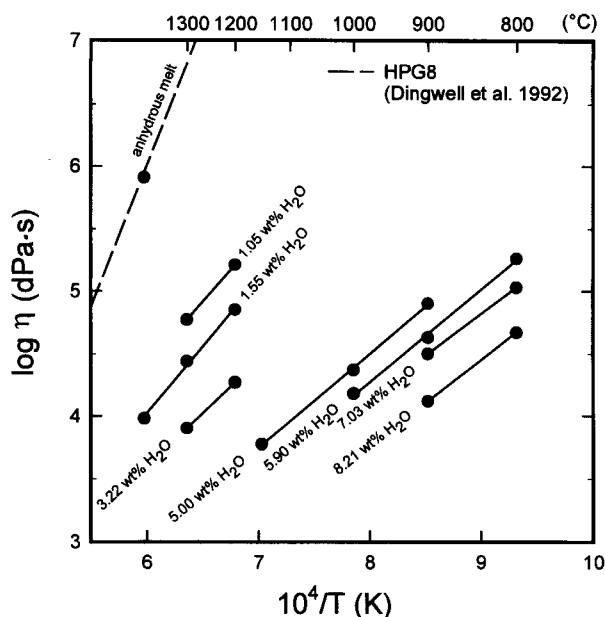


FIGURE 4. Viscosities of the hydrous AOQ melt vs. reciprocal absolute temperature. The slopes of the solid lines yield the activation energies of viscous flow, which are reported in Figure 5. Dashed curve is from Dingwell et al. (1992) for anhydrous melt.

similar to that obtained for anhydrous melts with decreasing polymerization (from metaluminous silicate melts to peralkaline melts, e.g., Bockris et al. 1955). However, comparisons between the effect of H₂O and alkali cations yield shortcomings, which were recently discussed by Hess et al. (1995). The main problems for such a comparison were as follows: (1) There were no data available on the effect of H₂O and alkali cations on melt viscosity for the same base composition; (2) the degree to which H₂O dissociates in the melt at P and T was unknown, and assumptions were made on the basis of measurements on quenched melts (e.g., Stolper 1982; Silver and Stolper 1989); and (3) the effect of pressure on the melt viscosities was difficult to quantify.

The results of this study in combination with those of Hess et al. (1995) on a similar melt composition (HPG8) allow direct comparison of the effects of H₂O and excess alkalis (Li, Na, K, Rb, Cs) on the viscosity of haplogranitic melts. Furthermore, new in situ spectroscopic data on H₂O speciation in AOQ melt (Nowak 1995; Nowak and Behrens 1995) allow reliable equilibrium constants for the dissociation reaction $\text{H}_2\text{O}_{\text{melt}} + \text{O}_{\text{melt}}^{2-} = 2 \text{OH}_{\text{melt}}^-$ to be calculated at a given temperature.

Figure 3 shows a comparison of our data and those of Hess et al. (1995) for HPG8 melts with excess alkalis. The viscosity is plotted as a function of the polymerization parameter NBO/T calculated after Persikov (1991). NBO/T expresses the ratio of nonbridging oxygen to tetrahedrally coordinated ions such as Si⁴⁺ and Al³⁺. The proportion of H₂O dissolved as OH⁻ was calculated with an equilibrium constant of 0.862 for 800 °C (Nowak 1995;

TABLE 3. Experimentally determined activation energies and preexponential coefficients of the investigated compositions

| Sample | E_a (kJ/mol) | $\log \eta_0$ (dPa·s) |
|-----------|----------------|-----------------------|
| AOQVis0 | (437)* | (-7.69)* |
| AOQVis1 | 195 | -1.71 |
| AOQVis1.5 | 181 | -1.60 |
| AOQVis2 | n.d. | n.d. |
| AOQVis2.5 | n.d. | n.d. |
| AOQVis3 | 164 | -1.55 |
| AOQVis4 | n.d. | n.d. |
| AOQVis5 | 144 | -1.53 |
| AOQVis6 | 142 | -1.64 |
| AOQVis7 | 134 | -1.19 |
| AOQVis8 | 133 | -1.78 |

Note: n.d. = not determined.

* Value taken from Dingwell et al. (1992) for HPG8 melt.

Nowak and Behrens 1995). In a first approximation molecular H₂O was assumed to have no influence on the viscosity of the melt. The effect of pressure on the viscosity was considered to be negligible as shown above (Fig. 2). The curve for the hydrous AOQ melt in Figure 3 was calculated using Equation 5 (see below). The viscosities for HPG8 with added alkalis were calculated with the fit parameters given by Hess et al. (1995) for the Vogel-Fulcher-Tammann equation. Hess et al. (1995) showed that the viscosity of the peralkaline melts increases with the size of the added cations in the order Li < Na < K, Rb, Cs. The comparison presented in Figure 3 shows clearly that H₂O is more effective than Li₂O in reducing the viscosity of the melt, suggesting that the viscosity of the melt is directly related to the radii or, better, to the electric-field strength of the monovalent cations. Thus, polarization of the T-O bonds by the cations facilitates the breaking of these bonds and the rearrangement of the network in response to applied stress.

Temperature dependence

The temperature dependence of the viscosity can be expressed as an Arrhenius function of reciprocal absolute temperature with the use of an equation of the form

$$\log_{10}\eta = \log_{10}\eta_0 + \frac{E_a}{2.303R} \cdot \frac{1}{T} \quad (3)$$

where η is the viscosity at temperature T (in kelvins), η_0 the preexponential factor, E_a (in kilojoules per mole) the activation energy of the viscous flow, and R the gas constant. It should be mentioned that the viscosity of silicate melts is not in general a linear function of reciprocal temperature (e.g., Richet 1984; Hummel and Arndt 1985). But within the restricted temperature range at which the data of this study were obtained ($\Delta T = 500$ °C) this relation can be considered as a valid approximation. The relationship $\log \eta$ vs. $1/T$ is presented in Figure 4. First-order regressions were used to calculate values for E_a and $\log \eta_0$ for each composition. The results are given in Table 3. A plot of E_a vs. H₂O content of the melt is shown in Figure 5.

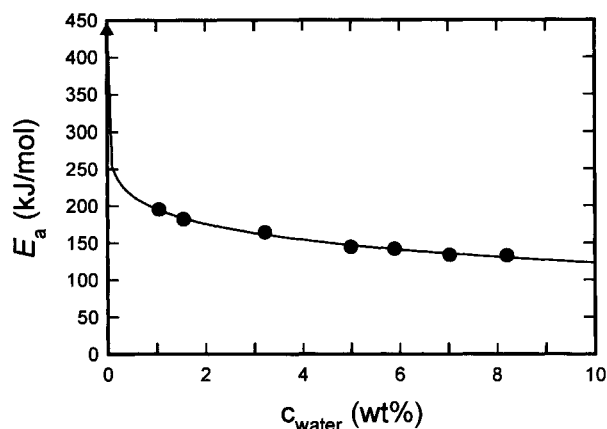


FIGURE 5. The activation energy of the viscous flow vs. H₂O content of the AOQ melt. The activation energy for the dry melt (triangle) is from Dingwell et al. (1992). The curve through the data was fitted with the power law given in Equation 4.1.

E_a shows a strong dependence on the H₂O content of the melt, especially for low H₂O concentrations. E_a decreases from 436 kJ/mol for the anhydrous melt to 195 ± 60 kJ/mol for a melt containing 1.05 wt% H₂O. The further addition of H₂O reduces the activation energy to 133 ± 30 kJ/mol for a melt with 8.21 wt% H₂O. The uncertainties for the E_a values for each composition (H₂O content) are high because only two to three viscosity values were available over a restricted temperature range. However, the general consistency of the whole data set suggests that the precision for E_a is better than that calculated for each composition separately. The compositional dependence of E_a (in kilojoules per mole) can be described with sufficient accuracy by a simple three-parameter power law:

$$E_a = 448.03 - 252.13[c_{\text{H}_2\text{O}}(\text{wt}\%)]^{0.11} \quad (4.1)$$

$$E_a = 448.38 - 236.2[c_{\text{H}_2\text{O}}(\text{mol}\%)]^{0.11} \quad (4.2)$$

where $c_{\text{H}_2\text{O}}$ is the H₂O concentration of the melt (mole percent is calculated on one O atom basis).

The values of $\log \eta_0$ are almost independent of the H₂O concentrations in the range 1–10 wt% H₂O (see Table 3) and vary from $10^{-1.18}$ to $10^{-1.78}$ dPa·s, with an average value of $10^{-1.57}$ dPa·s.

The experimentally determined values of E_a and $\log \eta_0$ were used to derive a function that enables the calculation of viscosities for hydrous AOQ melts at various H₂O contents and temperatures with a precision of ± 0.2 log units:

$$\log \eta = -1.57 + \{23.398 - 13.197[c_{\text{H}_2\text{O}}(\text{wt}\%)]^{0.11}\} \times 10^3 [1/T(\text{K})] \quad (5.1)$$

$$\log \eta = -1.57 + \{23.416 - 12.335[c_{\text{H}_2\text{O}}(\text{mol}\%)]^{0.11}\} \times 10^3 [1/T(\text{K})] \quad (5.2)$$

Figure 6 shows the correlation between the calculated and experimentally determined viscosities. It is emphasized

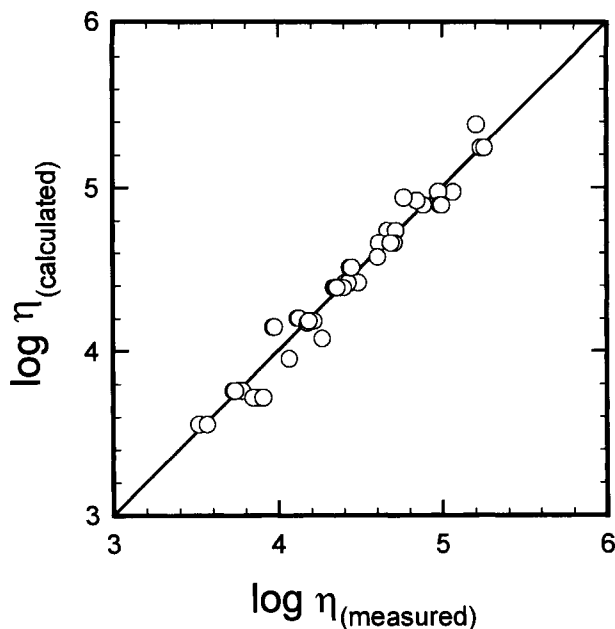


FIGURE 6. Correlation between measured and calculated viscosities with use of Equation 5. The agreement is always better than 0.2 log units.

that the parameters given in Equations 4.1 and 4.2 are empirical parameters and have no physical meaning.

Strictly, Equations 4 and 5 are valid only for the composition and H₂O range investigated in this study. However, it is emphasized that the effect of H₂O on the viscosity of albite melts is close to that observed for the AOQ composition of this study (Fig. 7a). This suggests that Equations 5.1 and 5.2 can be used to estimate the viscosities of other haplogranitic melts with compositions more albite-rich than AOQ within an error of ± 0.5 log units. Furthermore, viscosities predicted by Equations 5.1 and 5.2 are in good general agreement with measurements performed on natural granite compositions (Fig. 7b) and can be used in a first approximation to estimate the viscosities of natural hydrous peraluminous to metaluminous melts with 2–8 wt% H₂O. Extrapolation to higher H₂O contents may be possible because fundamental changes in the dependence of the viscosity on the H₂O content of the melt are not expected. More critical are viscosity calculations at H₂O concentrations between 0 and 1 wt% H₂O. Dramatic changes in viscosity and in the activation energy and preexponential coefficient in this concentration range are observed (Fig. 5 and Table 3). Without data on very low H₂O concentrations any calculation model would yield uncertainties that cannot be neglected.

COMPARISON WITH CALCULATION MODELS

The model of Shaw (1972)

Shaw (1972) considered that viscosity has an Arrhenian behavior and derived a simple method to calculate viscosities by simplifying the model of Bottinga and Weill

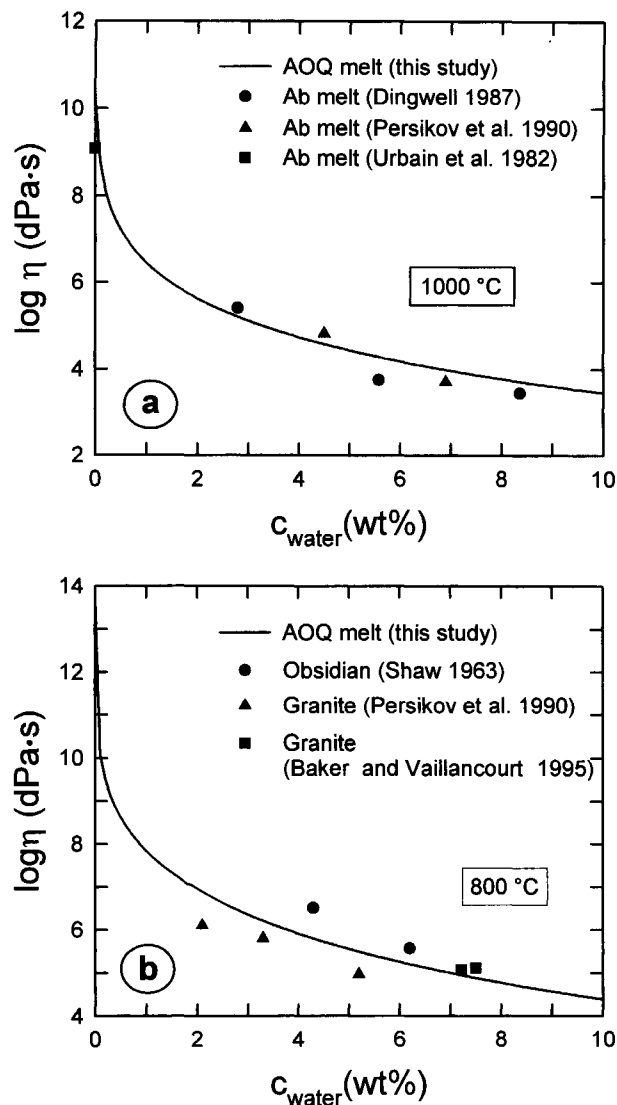


FIGURE 7. (a) Comparison between the viscosities of AOQ melts (curve) and the viscosities of albite melts as a function of H₂O content at a temperature of 1000 °C. Viscosities taken from Dingwell (1987) were measured at 7.5 kbar, from Persikov et al. (1990) at 2 and 6 kbar, and from Urbain et al. (1982) at 1 bar. (b) Comparison between the viscosities of AOQ melts (curve) and the viscosities of natural granitic melts as a function of H₂O content at a temperature of 800 °C. Viscosities taken from Baker and Vaillancourt (1995) were measured at 10 kbar, from Persikov et al. (1990) at 0.5, 1, and 2 kbar, and from Shaw (1963) at 1 and 2 kbar. H₂O content for granitic melts from Baker and Vaillancourt (1995) was taken as the sum of H₂O and F in the melt [see Baker and Vaillancourt (1995) for details].

(1972). Two principal assumptions were made by Shaw (1972): (1) In an Arrhenian plot, a viscosity curve for any given multicomponent mixture intersects the curve for SiO₂ liquid at the same point. The intersection of all viscosity curves at one point implies that the value for log η_0 is defined by only the slope of the curve. (2) For inter-

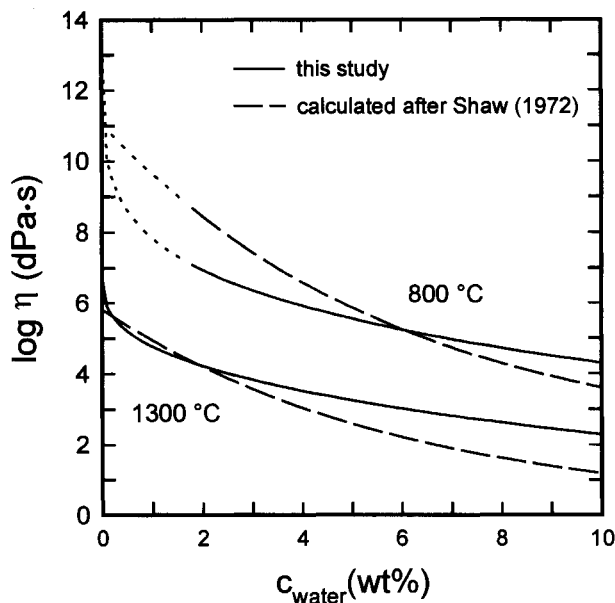


FIGURE 8. Comparison between the measured viscosities from this study and calculated viscosities for the AOQ melt from the model of Shaw (1972). The dashed parts of the 800 °C curves represent subliquidus conditions.

mediate compositions ($0.4 \leq X_{\text{SiO}_2} \leq 0.8$) the mean activation energy of a multicomponent mixture is given by the average of characteristic partial molar activation energies of SiO₂ in the pseudobinary SiO₂-oxide systems from which the multicomponent mixture can be deduced.

Because the model of Bottinga and Weill (1972) does not consider the effect of H₂O on melt viscosities, experimental data on the viscosity of hydrous molten obsidian (Shaw 1963) were used to estimate the partial molar activation energy of SiO₂ in the binary system SiO₂-H₂O. These data were obtained at only two H₂O concentrations (4.3 and 6.2 wt% H₂O) and in the temperature interval of 700–900 °C.

Figure 8 compares the measured viscosities of this study and the calculated viscosities for the AOQ composition with use of the model of Shaw (1972) for 800 and 1300 °C.

There is a good agreement between calculated and measured viscosities at 800 °C and H₂O concentrations between 4 and 7 wt% H₂O. At lower H₂O concentrations the model significantly overestimates the viscosities, whereas at higher H₂O concentrations the viscosities are underestimated. At 1300 °C no agreement is found for H₂O concentrations higher than 4 wt%. The agreement for low H₂O concentrations seems to be fortuitous. It was noted by Shaw (1972) that any empirical prediction model yields an averaging effect. By reducing the number of components in the system larger deviations between calculated and measured viscosities are expected. This is illustrated by the comparison of the calculated and measured viscosities for the dry melt, where the deviations can be as large as two orders of magnitude (Fig. 8).

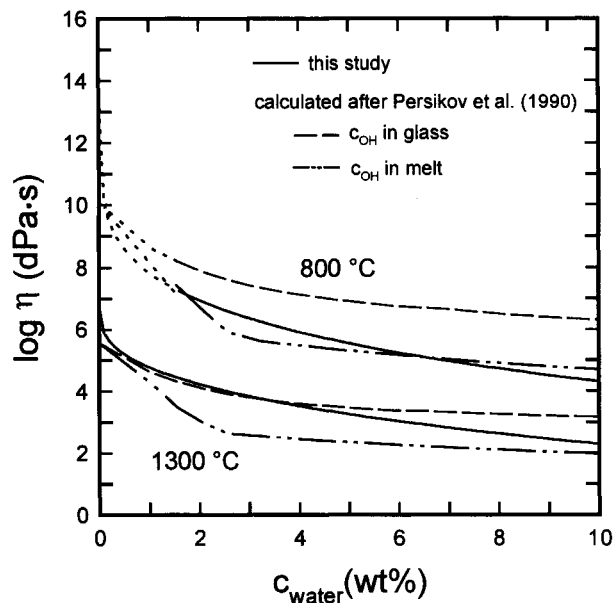


FIGURE 9. Comparison between the measured viscosities from this study and calculated viscosities for the AOQ melt from the model of Persikov et al. (1990). The dashed parts of the 800 °C curves represent subliquidus conditions. See text for further details on the assumed H₂O speciation.

The model of Persikov et al. (1990)

The model of Persikov et al. (1990) was developed on the basis of viscosity measurements made with the falling-sphere method in a specially designed *in situ* viscosimeter. Viscosities were measured on synthetic NaAl-Si₃O₈ melt and on natural melts with granitic to tholeiitic compositions, and with the addition of H₂O (0.00–12.3 wt%), HF, and HCl.

Like Shaw (1972), Persikov et al. (1990) derived their model from an Arrhenian equation. The main features of the model are as follows: (1) The preexponential coefficient η_0 is a constant (numerical value $\log \eta_0 = -3.5$) and therefore independent of melt composition. (2) The activation energy, E_a , is dependent on the degree of polymerization of the melt. The degree of polymerization is characterized by the parameter $K = 100\text{NBO}/T$. Persikov et al. (1990) found a regular decrease in activation energy in the sequence acidic to ultramafic melts. This sequence is divided into four compositional ranges expressing different polymerization states of the melt. For each range the activation energy for the viscous flow is calculated with a separate equation. Furthermore, a piezocoefficient is applied to consider the dependence of the melt viscosity on the lithostatic (total) pressure. The model takes into account the existence of two H₂O species in hydrous melts. OH⁻ groups are considered as network modifiers, whereas the influence of molecular H₂O on the activation energy, which is assumed to be lower, is calculated separately. A detailed example of the calculation procedure is given by Persikov (1991).

Figure 9 compares the measured viscosities and the

calculated viscosities for the AOQ composition with use of the model of Persikov et al. (1990) for 800 and 1300 °C. The calculations were performed with two assumptions: (1) The degree to which H₂O dissociates to OH⁻ groups in the melt is the same as that determined at room temperature by near-IR spectroscopy on hydrous AOQ glasses with various H₂O concentrations (Nowak 1995; Nowak and Behrens 1995). (2) The ratio of OH⁻ to molecular H₂O existing in the melt at high *P* and *T* is calculated from in situ measurements (Nowak 1995; Nowak and Behrens 1995). The equilibrium constants *K*₁ for the reaction H₂O_m + O_m²⁻ = 2 OH_m⁻ (*m* = melt) at 800 and 1300 °C are 0.862 and 2.824, respectively, leading to an OH⁻ concentration that is significantly higher than that found in the quenched melt.

At 800 °C fairly good agreement is reached by calculating the viscosities with the proportion of OH⁻/H₂O obtained using the equilibrium constant *K*₁ = 0.862. The highest deviation is about one order of magnitude with H₂O content of 3 wt%. At higher temperatures a significant deviation is observed in the case of the OH⁻/H₂O ratio calculated with the equilibrium constant *K*₁ = 2.824. Better agreement is obtained if the OH⁻/H₂O ratios found in spectroscopic investigations of quenched melts are considered. However, this is not surprising because the model of Persikov et al. (1990) was developed on the basis of H₂O speciation data derived from room-temperature measurements. In situ measurements of the H₂O speciation of hydrous melts (Nowak 1995; Nowak and Behrens 1995) clearly show that with increasing temperature the amount of H₂O decreases and that OH⁻ groups become the dominant species. This should be considered in a refinement of the model of Persikov et al. (1990). The significant deviations observed for almost dry melts (*K* = 0) are probably related to an inappropriate value for the activation energy of the dry melt. Persikov et al. (1990) suggested that the variation of the activation energy for melts with *K* = 0–17 is proportional to the ratio $\epsilon = \frac{[{}^{41}\text{Al}]}{[{}^{41}\text{Al}] + [{}^{41}\text{Si}]}$. However, no information was given on how to account for ϵ in the calculation of melt viscosities. The model as published by Persikov et al. (1990) uses the activation energy of albite melts for the calculation of viscosities of melts with *K* = 0–17. The activation energy for the dry haplogranitic melt is significantly higher (*E*_a = 439 kJ/mol; Dingwell et al. 1992) than that of albite melts (*E*_a = 292 kJ/mol; Persikov et al. 1990), which may explain the strong deviations observed for melts with H₂O contents <0.2 wt% H₂O.

CONCLUSIONS

The experimental results of this study have implications for the estimation of the viscosities of natural granitic and rhyolitic hydrous melts. In particular it has been shown that the variation in viscosity is more pronounced than that predicted by calculation models (Shaw 1972; Persikov et al. 1990) for low H₂O concentrations of the melt (<2 wt% H₂O). For melts with low H₂O concentrations such as observed in volcanic processes (low pressure

and degassing) neither model adequately describes the viscous behavior of the melts. More viscosity measurements at low H₂O concentrations are required to improve predictions.

In granitic or rhyolitic rocks formed at temperatures lower than 800 °C, the determined melt-H₂O contents in the ascending magmas have been found to be relatively elevated (4–7 wt% H₂O; e.g., Clemens 1984; Scaillet et al. 1995). Our results show that, in this range of temperature and H₂O content, strong deviations between experimentally determined and calculated viscosities are not expected using the model of Shaw (1972). Therefore, the viscosities of granitic melts can probably be predicted with a maximum uncertainty of ±0.5 log units with use of the model of Shaw (1972). The viscosities of peraluminous leucogranitic melts with high H₂O contents (>4 wt% H₂O; Baker and Vaillancourt 1995; Scaillet et al., in preparation) are also in good agreement with the model of Shaw (1972). The model of Persikov et al. (1990) is difficult to test and to use as long as sufficient in situ data on the H₂O speciation are unavailable.

ACKNOWLEDGMENTS

This work was supported by Procope (German-French research program no. 93018 between Hanover and Orléans). Technical assistance was provided by O. Dietrich, W. Hurkuck, and A. Lefèvre. We thank R.A. Lange and D.R. Baker for their helpful review of the manuscript.

REFERENCES CITED

- Baker, D.R., and Vaillancourt, J. (1995) The low viscosities of F + H₂O-bearing granitic melts and implications for melt extraction and transport. *Earth and Planetary Science Letters*, 132, 199–211.
- Behrens, H. (1995) Determination of water solubilities in high-viscosity melts: An experimental study on NaAlSi₃O₈ and KAlSi₃O₈ melts. *European Journal of Mineralogy*, 7, 905–920.
- Bockris, J.O'M., Mackenzie, J.D., and Kitchener, J.A. (1955) Viscous flow in silica and binary liquid silicates. *Transactions of the Faraday Society*, 51, 1734–1748.
- Bottlinga, Y., and Weill, D.F. (1972) The viscosity of magmatic liquids: A model for calculations. *American Journal of Science*, 272, 438–475.
- Burnham, C.W. (1964) Viscosity of a water rich pegmatite melt at high pressure. *Geological Society of America Special Papers*, 76, 26.
- Clemens, J.D. (1984) Water contents of silicic to intermediate magmas. *Lithos*, 17, 273–287.
- Dingwell, D.B. (1987) Melt viscosities in the system NaAlSi₃O₈-H₂O-F₂O₋₁. In B.O. Mysen, Ed., *Magmatic processes: Physicochemical principles*. Geochemical Society Special Publication, 1, 423–433.
- Dingwell, D.B., and Mysen, B.O. (1985) Effects of water on the viscosity of albite melt at high pressure: A preliminary investigation. *Earth and Planetary Science Letters*, 74, 266–274.
- Dingwell, D.B., Knoche, R., Webb, S.L., and Pichavant, M. (1992) The effect of B₂O₃ on the viscosity of haplogranitic liquids. *American Mineralogist*, 77, 457–461.
- Faxen, H. (1923) Die Bewegung einer starren Kugel längs der Achse eines mit zäher Flüssigkeit gefüllten Rohres. *Arkiv för Matematik, Astronomi och Fysik*, 17(27), 1–28.
- Friedman, I., Long, W., and Smith, R.L. (1963) Viscosity and water content of rhyolite glass. *Journal of Geophysical Research*, 68, 6523–6535.
- Goranson, R.W. (1938) Silicate-H₂O systems: Phase equilibria in the NaAlSi₃O₈-H₂O and KAlSi₃O₈-H₂O systems at high pressures and temperatures. *American Journal of Science*, 35, 71–91.
- Hazen, R.M., and Sharpe, M.R. (1983) Radiographic determination of the position of platinum spheres in density-viscosity studies of silicate melts. *Carnegie Institution of Washington Year Book*, 82, 428–430.

- Hess, K.-U., Dingwell, D.B., and Webb, S.L. (1995) The influence of excess alkalis on the viscosity of a haplogranitic melt. *American Mineralogist*, 80, 297–304.
- Holtz, F., Behrens, H., Dingwell, D.B., and Taylor, R.P. (1992) Water solubility in aluminosilicate melts of haplogranitic compositions at 2 kbar. *Chemical Geology*, 96, 289–302.
- Holtz, F., Behrens, H., Dingwell, D.B., and Johannes, W. (1995) H₂O solubility in haplogranitic melts: Compositional, pressure, and temperature dependence. *American Mineralogist*, 80, 94–108.
- Hummel, W., and Arndt, J. (1985) Variation of viscosity with temperature and composition in the plagioclase system. *Contributions to Mineralogy and Petrology*, 90, 83–92.
- Kohn, S.C., Dupree, R., and Smith, M.E. (1989) A multinuclear resonance study of the structure of hydrous albite glass. *Geochimica et Cosmochimica Acta*, 53, 2925–2935.
- Kushiro, I. (1978a) Density and viscosity of hydrous calc-alkalic andesite magma at high pressure. *Carnegie Institution of Washington Year Book*, 77, 675–677.
- (1978b) Viscosity and structural changes of albite (NaAlSi₃O₈) melt at high pressures. *Earth and Planetary Science Letters*, 41, 87–90.
- Lapham, K.E., Holloway, J.R., and Delaney, J.R. (1984) Diffusion of H₂O and D₂O in obsidian at elevated temperatures and pressures. *Journal of Non-Crystalline Solids*, 67, 179–191.
- Nowak, M. (1995) Der Einbau von Wasser in haplogranitischen Gläsern und Schmelzen. Ph.D. thesis, University of Hannover, Germany.
- Nowak, M., and Behrens, H. (1992) Water diffusion in albite and haplogranitic melts. *Terra Abstracts*, 4, 31.
- (1995) The speciation of water in haplogranitic glasses and melts determined by in situ near infrared spectroscopy. *Geochimica et Cosmochimica Acta*, 59, 3445–3450.
- Persikov, E.S. (1991) The viscosity of magmatic liquids: Experiment, generalized patterns: A model for calculation and prediction: Applications. In *Advances in Physical Geochemistry*, 9, 1–40.
- Persikov, E.S., Zharikov, V.A., Bukhtiyarov, P.G., and Polskoy, S.F. (1990) The effects of volatiles on the properties of magmatic melts. *European Journal of Mineralogy*, 2, 621–642.
- Petford, N., Kerr, R.C., and Lister, J.R. (1993) Dike transport of granitoid magmas. *Geology*, 21, 845–848.
- Puziewicz, J., and Johannes, W. (1988) Phase equilibria and compositions of Fe-Mg-Al minerals and melts in water saturated peraluminous granitic systems. *Contributions to Mineralogy and Petrology*, 100, 156–168.
- Richet, P. (1984) Viscosity and configurational entropy of silicate melts. *Geochimica et Cosmochimica Acta*, 48, 471–483.
- Roux, J., Holtz, F., Lefèvre, A., and Schulze, F. (1994) A reliable high-temperature setup for internally heated pressure vessels: Applications to silicate melt studies. *American Mineralogist*, 79, 1145–1149.
- Sabatier, G. (1956) Influence de la teneur en eau sur la viscosité d'une rétinite, verre ayant la composition chimique d'un granite. *Comptes Rendus de l'Académie des Sciences de Paris*, 242, 1340–1342.
- Sawyer, E.W. (1994) Melt segregation in the continental crust. *Geology*, 22, 1019–1022.
- Scailliet, B., Pichavant, M., and Roux, J. (1995) Experimental crystallization of leucogranite magmas. *Journal of Petrology*, 36, 663–705.
- Shaw, H.R. (1963) Obsidian-H₂O viscosities at 100 and 200 bars in the temperature range 700° to 900 °C. *Journal of Geophysical Research*, 68, 6337–6342.
- (1972) Viscosities of magmatic liquids: An empirical method of prediction. *American Journal of Science*, 272, 870–893.
- Silver, L., and Stolper, E.M. (1989) Water in albite glasses. *Journal of Petrology*, 30, 667–710.
- Stolper, E. (1982) Water in silicate glasses: An infrared spectroscopic study. *Contributions to Mineralogy and Petrology*, 81, 1–17.
- Tuttle, O.F., and Bowen, N.L. (1958) Origin of granite in the light of experimental studies in the system NaAlSi₃O₈-KAlSi₃O₈-SiO₂-H₂O. *Geological Society of America Memoir*, 74, 1–154.
- Urbain, G., Bottinga, Y., and Richet, P. (1982) Viscosity of liquid silica, silicates and aluminosilicates. *Geochimica et Cosmochimica Acta*, 46, 1061–1072.
- Watson, E.B. (1994) Diffusion in volatile-bearing magmas. In *Mineralogical Society of America Reviews in Mineralogy*, 30, 371–411.
- Weast, R.C., Astle, M.J., and Beyer, W.H. (1984) *CRC handbook of chemistry and physics* (64th edition), p. B-120. CRC Press, Boca Raton, Florida.
- White, B.S., and Montana, A. (1990) The effect of H₂O and CO₂ on the viscosity of sanidine liquid at high pressures. *Journal of Geophysical Research*, 95, 15683–15693.

MANUSCRIPT RECEIVED JULY 14, 1995

MANUSCRIPT ACCEPTED MAY 6, 1996